ACS APPLIED MATERIALS & INTERFACES

Research Article

www.acsami.org

Local and Sustained Gene Delivery in Silica-Collagen Nanocomposites

Xiaolin Wang, Christophe Hélary,* and Thibaud Coradin*

Sorbonne Universités, UPMC Univ Paris 06, CNRS, Collège de France, UMR 7574, Chimie de la Matière Condensée de Paris, F-75005, Paris, France

Supporting Information

ABSTRACT: Local delivery of biomolecules from hydrogels is highly challenging because of their rapid diffusion and degradation. Gene therapy represents an alternative that allows for the prolonged production of proteins by transfected cells. In this study, we have developed nanocomposites consisting of DNA-polyethylenimine-silica nanoparticle complexes coencapsulated with fibroblasts within collagen hydrogels. Through the modulation of the particle size and polyethylenimine molecular weight, it was possible to achieve "in-gel" transfection permitting the sustained production of biomolecules from hydrogels over 1 week. Alternative configurations consisting of particle addition to cellularized gels and cell culture in the presence of complex-containing hydrogels were also investigated. These studies demonstrated that particle encapsulation limits DNA and silica dissemination outside the collagen hydrogels. They also show the key role of cell proliferation within collagen hydrogels on the transfection efficiency. Such nanocomposites therefore constitute promising materials for the development of novel gene delivery systems to promote tissue repair.

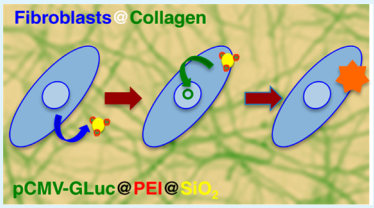

KEYWORDS: *gene delivery, collagen, silica nanoparticles, nanocomposites, tissue engineering*

INTRODUCTION

Healing requires a well-orchestrated integration of biological events that lead to tissue repair.[1] In some cases, tissue repair is impaired due to a chronic inflammation, a fibrosis, or a large defect of tissue.[2,3] These pathophysiological situations require the treatment of wounds. Protein therapies have first been developed with the aim of favoring tissue regeneration.[4,5] Despite the effort in the development of drug delivery systems, protein therapies suffer from high cost, rapid diffusion, and degradation of biomolecules.[6] An alternative strategy relies on the implantation of biomaterials into the wound site.[7] Scaffolds have to provide biophysical and biochemical signals to guide the formation of neo-tissue at the site of injury.[6] Nowadays research orientation is toward the integration of active biomolecules within scaffolds in order to tune cell phenotype toward migration, differentiation, or modulation of inflammation.[2]

Gene therapy represents a promising alternative to protein delivery as it overcomes the concerns about protein stability and affords a sustained delivery of biomolecules.[8] Gene delivery into cells makes them produce therapeutic molecules that act locally, thereby preventing harmful side effects.[9] Success of gene delivery depends on the development of an efficient delivery vector that permits the penetration of genes into the cells as well as their protection against endosomal degradation. Viruses are the most efficient vectors to transfect cells but they suffer from safety concerns such as immunogenicity or oncogenicity.[10,11] Polymers such as dendrimers are an alternative as they allow the conjugation of large DNA molecules with low toxicity.[12,13] Among the nonviral vectors, polyethylenimine (PEI) has emerged for gene transfection. PEI is able to compact large DNA sequences such as plasmids and permits DNA penetration into cells thanks to its positive charge.[14] In addition, PEI is able to escape from the endosome due to the "proton-sponge" effect.[15] As the efficiency and toxicity are strongly correlated with the molecular weight, efforts have been made to explore the possibility of applying PEI with lower molecular weight by chemical modification[16] or complexation with nanoparticles[17] to shield their positive charge.

In this context, silica nanoparticles (SiNP) possess several attractive characteristics such as biocompatibility, large surface area, tunable size/shape, and versatile bioconjugation chemistry[18] making them ideal drug delivery vehicles[19] and gene-transfection agents.[20] Nevertheless, regular SiNPs, being plain or mesoporous (MSN), cannot be used alone as gene carriers as they bear a negative charge near neutral pH and are unable to compact DNA, thereby preventing its internalization.[21] Several studies have been performed to modify SiNP with PEI by in situ polymerization,[22] covalent bonding,[23] and electrostatic adsorption.[24] The latter option appears particularly attractive to enhance transfection but has so far been evaluated mainly on MSN systems.

In tissue engineering, encapsulation of gene cargo within a scaffold is crucial to get a prolonged effect within the wound site. First, gene carriers are more effective when they are immobilized, as the host material can control their release.[25] Second, scaffolds have an effect in wound healing on their own.

Received: October 24, 2014
Accepted: January 8, 2015
Published: January 8, 2015

© 2015 American Chemical Society

DOI: 10.1021/am507389q
ACS Appl. Mater. Interfaces 2015, 7, 2503−2511

Scheme 1. Schematic Representation of the Three Models Used in This Study

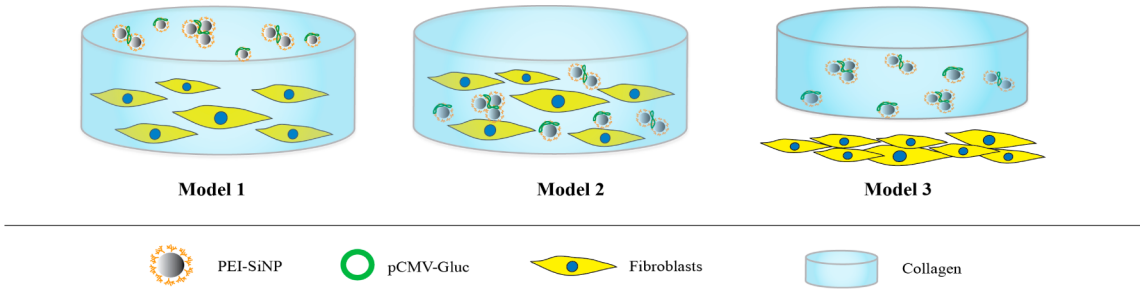

In particular, collagen-based materials give the right signal to cells for adhesion, migration, and proliferation.[26,27] Moreover, they provide appropriate hydration and can be remodeled by host cells. Type 1 collagen is one of the most extensively investigated polymers for scaffold-mediated gene delivery. For local gene therapy, combining scaffolds and polyplexes (i.e., DNA-polymer complexes) has been investigated.[28] Polyplexes are either dropped at the material surface after its formation or encapsulated during scaffold preparation.[29] The first technique leads to a low DNA loading and a rapid diffusion, whereas the second often leads to polyplex aggregation and inactivation.

In this study, collagen-based nanocomposite hydrogels integrating plain silica nanoparticles were evaluated as gene delivery systems to favor tissue repair. Such materials were previously shown to be biocompatible after subcutaneous implantation in rats.[30] It was also recently demonstrated that the collagen hydrogel provides a suitable environment to slow down the release of antibiotics entrapped in plain SiNPs.[31] On this basis, we hypothesized that the integration of plasmid-PEI-SiNP complexes within collagen hydrogels would allow for a sustained gene release. We show here that PEI-coated silica nanoparticles with optimal size and polymer molecular weight are efficient plasmid vectors when they are entrapped within cellularized collagen networks, allowing for a prolonged gene expression. We demonstrate that the transfection efficiency depends on both particle diffusion and cell proliferation within the hydrogel. The encapsulation of the vectors within the protein scaffold also has the advantage of avoiding rapid dissemination of the plasmids and the particles, providing a safe solution for the development of biofunctional medical dressings favoring tissue regeneration.

EXPERIMENTAL SECTION

Preparation and Functionalization of Silica Nanoparticles. Silica nanoparticles (SiNP) with diameter d varying from 50 to 400 nm were synthesized by the Stöber method using ammonia, ethanol, and tetraethylorthosilicate (TEOS) (see Table S1 in the Supporting Information). The as-synthesized particles were dialyzed against distilled water for 2 days, recovered by centrifugation, and resuspended in 10 mM phosphate buffer saline (PBS) (pH = 7.4). For PEI-SiNP particle preparation, 200 mg of branched PEI with different molecular weights (1.8 kDa, 10 kDa, 25 kDa, Sigma-Aldrich) was dissolved in 20 mL of 10 mM PBS (pH 7.4). Silica nanoparticle suspension (20 mL) with the same concentration was then added dropwise into the PEI solution under stirring. The mixtures were further stirred for 48 h after which particles were recovered by centrifugation, washed 3 times in 10 mM PBS, and finally resuspended in the buffer solution. Particle sizes and zeta potentials (ζ) were measured in 10 mM PBS solution using a ZetaSizer Nano (Malvern Instruments Ltd., Worcestershire, UK). Particles were also imaged using transmission electron microscopy (TEM) on a JEOL 1011 instrument. The amount of adsorbed PEI was determined by thermogravimetric analysis (TGA) and elemental analysis (C,H,O,N).

pDNA-PEI and pDNA-PEI-SiNP Complexation. Reporter plasmid pCMV-GLuc (pGluc) encoding Gaussia Luciferase (New England BioLabs, Ipswich, MA) was used to quantify transgene expression. This plasmid was amplified by one shot BL21(DE3) pLysS kit (Invitrogen, Life technologies), extracted by one PureLink HiPure Plasmid kit (Invitrogen, Life technologies), and finally stored in Tris-EDTA buffer at −20 °C. pDNA-PEI complexes were prepared at weight ratio of 1:2. pDNA-PEI-SiNP complexes were prepared at various pDNA:PEI-SiNP weight ratios. Complex formation was examined by agarose gel electrophoresis. Briefly, 1 μL of pDNA solution (0.1 $\mu g.\mu L^{-1}$) was mixed homogeneously with a total volume of 9 μL of PEI-SiNP suspension or PEI solution (PBS 1×) by vortexing in a microcentrifuge tube. The resulting mixtures were left at room temperature for 2 h to achieve complete complexation, before being loaded onto 0.7% agarose gel with ethidium bromide (0.1 $\mu g.mL^{-1}$) and running with TAE buffer at 100 V for 40 min. DNA retardation was observed by irradiation with ultraviolet light.

Fibroblast Cell Culture. 3T3 mouse fibroblasts were cultured in complete cell culture medium (Dulbecco's Modified Eagle's Medium (DMEM) supplemented with 10% fetal serum, 100 $U.mL^{-1}$ penicillin, 100 $\mu g.mL^{-1}$ streptomycin, and 0.25 $\mu g.mL^{-1}$ Fungizone). Tissue culture flasks (75 cm^2) were kept at 37 °C in a 95% air:5% CO_2 atmosphere. Before confluence, fibroblasts were removed from culture flasks by treatment with 0.1% trypsin and 0.02% EDTA. Cells were rinsed and resuspended in the above culture medium before use.

Preparation of Collagen-Based Nanocomposites. Collagen type I was purified from rat tails and the concentration was estimated by hydroxyproline titration, as previously described. Tubes separately filled with collagen solution (2 $mg.mL^{-1}$ in 17 mM acetic acid), whole cell culture medium, and 0.1 M NaOH were kept in ice bathes for 1 h before preparation to slow down the gelling kinetics of collagen. Complexes were formed by adding 1 μg of pDNA to 25 μL of a solution containing PEI or PEI-SiNP in order to achieve the pDNA:PEI (or pDNA-PEI-SiNP) ratio obtained from gel electrophoresis. Three models were proposed in our study: particles on top of cellularized hydrogels (model 1), co-entrapped particles and cells (model 2), and cells beneath free-floating nanocomposites (model 3) (Scheme 1). For model 1, 500 μL of collagen solution and 400 μL of culture medium were added to a 1.5 mL tube and vortexed vigorously. After addition of 30 μL of 0.1 M NaOH and strong vortexing, 125 μL of the cell suspension at a density of 10^6 $cells.mL^{-1}$ was added and mixed homogeneously. Then 0.9 mL was sampled from the mixture and deposited onto a 24-well plate. The plate was then incubated at room temperature for 10 min for complete gelling of collagen. After this delay, 25 μL of the complex solution was added onto the surface of the materials. For model 2, a similar procedure was followed except that the 25 μL of complexes was mixed with 100 μL of the cell suspension before gel formation. Model 3 was similar to model 2 except that the cell suspension was replaced by culture medium and the recovered hydrogels were left free-floating in the culture medium of plate-seeded cells (5×10^3 $cells.mL^{-1}$).

Cell Transfection and Cell Viability. Transfection efficiency of pDNA-PEI and pDNA-PEI-SiNP were evaluated by luciferase expression of pGLuc by 3T3 fibroblast cells in cell culture medium.

DOI: 10.1021/am507389q
ACS Appl. Mater. Interfaces 2015, 7, 2503−2511

To perform cell transfection in 2D, 3T3 mouse fibroblasts were plated at a density of 5×10^4 per well in a 24-well plate. pDNA-PEI or pDNA-PEI-SiNP complexes (25 μL, prepared as described above) were added to the cell culture medium. After 4 h, the supernatant was removed, the well was refreshed with 1 mL medium, and the cells were then cultured for another 44 h in complete medium for the expression of luciferase. To perform cell transfection in 3D, pDNA complexes were added on the top of the hydrogel (model 2) or mixed with the collagen solution (model 1 and 3). One milliliter of whole medium was then added in each well. At selected time points over a 1-week period, 0.5 mL of the culture medium was collected from the wells and replenished with equal volumes of fresh medium. For measurements of luciferase activity, a BioLux Gaussia Luciferase Assay Kit (New England Biolabs) was used and transgene expression of luciferase was reported as relative light units (RLU). Control groups were under the same culture condition as the experiment groups except for the absence of DNA complexes.

Internalization of nanoparticles in 3T3 mouse fibroblasts was studied using fluorescence microscopy. For cells cultured in 2D, the pDNA-particle complexes along with cell culture medium were removed after 24 h incubation, rinsed 3 times with PBS, and fixed with 4% paraformaldehyde for 1 h at RT. The cell nucleus was then stained with DAPI (4′,6-diamidino-2-phenylindole dihydrochloride, Life technologies, 300 nM in PBS) for 10 min and rinsed with PBS before observation. For cells immobilized in collagen hydrogels, gels were incubated for 48 h, rinsed 3 times with PBS, and fixed with 4% paraformaldehyde overnight. Next, the fixed samples were dehydrated in ethanol and butanol and incorporated in paraffin to obtain 10 μm histological sections with a manual microtome. Before observation, the as-obtained samples were immersed in toluene, ethanol, and then water for rehydration. The cell nucleus was stained with DAPI for 10 min and rinsed with PBS before observation. Model 2 was also studied by scanning electron microscopy (SEM). Collagen hydrogels were fixed using 3.63% glutaraldehyde in a cacodylate/saccharose buffer (0.05 M /0.3 M, pH 7.4) for 1 h at 4 °C. Following fixation, samples were washed three times in a cacaodylate/saccharose buffer (0.05 M /0.3 M, pH 7.4) and dehydrated through successive increasing concentration ethanol baths from 70% to 100% alcohol. Thereafter, samples were dried in a critical point dryer and gold sputtered (20 nm) for analysis. Samples were observed with Hitachi S-3400N SEM operating at 10 kV.

Cell viability was monitored using the Alamar Blue test. For the 2D model, cell culture medium was removed for luciferase activity test and 200 μL of the Alamar Blue solution (10% in cell culture medium) was added. The cells were then incubated at 37 °C with 5% CO_2 for 4 h. The supernatant in each well was then collected, diluted with 800 μL water, and its absorbance measured at λ = 570 and 600 nm. Cell viability was calculated and reported as a percentage of the control group (n = 3 or 6). For the 3D model, cell viability was assessed in the same way except that the 800 μL water was first added to the collagen gel for 0.5 h at room temperature to extract the Alamar blue solution trapped in the gel and then collected for the absorbance measurements. To further understand the proliferation of cells in the collagen gel (1 mg/mL) over 1 week, cell viability was evaluated with the Alamar Blue test as described before on 2, 5, and 7 d, respectively, and was calculated as the percentage of that at 2 d.

Statistical Analysis. Graphical results are presented as mean ± SD (standard deviation). Statistical significance was assessed using one-way analysis of variance (ANOVA) followed by Tukey (compare all pairs of groups) or Dunnett (compare a control group with other groups) posthoc test. The level of significance in all statistical analyses was set at a probability of $P < 0.05$.

RESULTS AND DISCUSSION

Effect of Silica Nanoparticle Size on Fibroblast Transfection in 2D. Plain silica nanoparticles $SiNP_d$ with diameters ranging from 50 to 400 nm were obtained using the Stöber reaction, as indicated by DLS measurements in water (Table 1) and confirmed by TEM observation (Figure S1 of the Supporting Information). Zeta potential (ζ) values were constant over the particle size variation and significantly negative (−25/−35 mV), as expected for silica near neutral pH. After contact with PEI_{25}, all particles have a positive ζ value in PBS, in agreement with the surface deposition of the polycation polymer. The amount of adsorbed PEI was maximum for $SiNP_{50}$ and $SiNP_{200}$ particles (ca. 15 w%) and lower for $SiNP_{100}$ and $SiNP_{400}$. DLS studies indicate that particles with intermediate sizes have a good stability in PBS whereas the smallest and largest ones show a tendency toward aggregation.

Table 1. Diameter (d) and Zeta Potential (ζ) and PEI Amount for Silica Nanoparticles before and after Coating with PEI-25 kDa

bare particles		after coating		
d_{H2O} [nm][a]	ζ_{H2O} [mV]	d_{PBS} [nm][a]	ζ_{PBS} [mV]	PEI [wt %][b]
50 ± 10	- 28 ± 12	140 ± 70	+ 18 ± 8	15
120 ± 20	- 27 ± 11	150 ± 40	+ 19 ± 6	10
210 ± 10	−26 ± 8	250 ± 40	+ 19 ± 6	15
390 ± 40	−35 ± 7	420 ± 150	+ 20 ± 9	5

[a]From DLS. [b]±2 wt %, from TGA.

The complexation ability of the different PEI_{25}-coated $SiNP_d$'s was studied by electrophoretic mobility shift assays of pDNA (Figure 1). The optimal plasmid:particle weight ratio ensuring full retention of pDNA by particles was 1:30 w/w% for $SiNP_{400}$ and $SiNP_{200}$ and 1:10 w/w% ratio for $SiNP_{100}$ and $SiNP_{50}$.

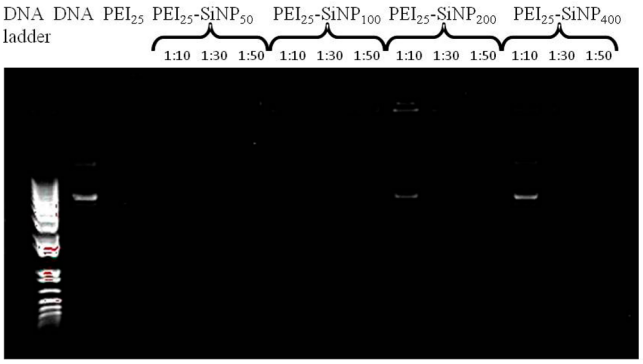

Figure 1. Agarose gel electrophoresis showing the particle size effect on pDNA complexation by $PEI_{25}SiNP_d$. A constant amount of DNA was complexed with silica particles at different weight ratios 1:10, 1:30, and 1:50.

The cell transfection ability of these complexes was studied on 3T3 fibroblast cells seeded in 24-well plates (2D configuration). Luciferase expression, indicative of successful internalization and transport to the nucleus of the pDNA, was observed for all systems (Figure 2). Importantly, PEI_{25}, pDNA, and $SiNP_d$ alone gave no significant signal. The PEI_{25} polymer alone was the most efficient transfecting agent, whereas its adsorption on SiNP decreases its transfection ability by 1 order of magnitude regardless of the nanoparticle size. This may be attributed to the fact that a fraction of the positively charged ammonium groups of PEI is interacting with the silica surface and is therefore no longer accessible for DNA complexation. Another explanation is related to the size of the complexes that can be less adequate for cell internalization by fibroblasts than PEI alone. Fibroblasts are able to internalize particles by

DOI: 10.1021/am507389q
ACS Appl. Mater. Interfaces 2015, 7, 2503−2511

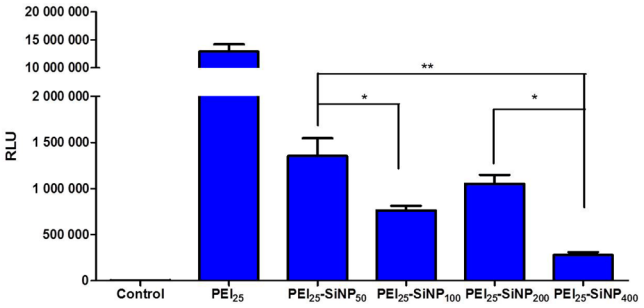

Figure 2. Transfection of 3T3 mouse fibroblasts after 4 h incubation with free and silica-associated PEI_{25} expressed in relative light units (RLU) (n = 3). Variance of the luciferase expression among groups PEI_{25}–$SiNP_{50}$, PEI_{25}–$SiNP_{100}$, PEI_{25}–$SiNP_{200}$ and group PEI_{25}–$SiNP_{400}$ was determined by one-way ANOVA with Tukey posthoc test (*P < 0.05, ** P < 0.01).

endocytosis in a size dependent manner, with smaller particles being more rapidly engulfed by cells than larger ones.[32] Noticeably, internalization of nanoparticles with a diameter larger than 500 nm is observed only in exceptional cases.[33] PEI_{25} on its own has the best ability to compact DNA and generate 100 nm complexes suitable for cell uptake.[14] In contrast, after PEI adsorption, SiNPs have diameters in the 150–420 nm range. This can explain why the largest PEI_{25}–$SiNP_{400}$ exhibited the lowest transfection efficiency.

Considering the effect of particle size in more detail, it is worth pointing out that adsorption of cationic polyelectrolytes on silica surface is a complex phenomenon where transitions from flat to extended configurations are observed as a function of polymer concentration. The particle size also has a major influence on the adsorption process from different points of view: it controls the density of silanol groups, and therefore particle surface charge; it dictates the available surface for adsorption per particle; it defines the maximum packing density of polymers via its radius of curvature. Here a reliable comparison must be made from the PEI density on the particle surface rather than the amount of PEI sorption per gram of silica. Such a density can be estimated by the product of PEI wt % by particle radius, leading to PEI density decreasing as $SiNP_{200}$ > $SiNP_{400}$ > $SiNP_{100}$ > $SiNP_{50}$. It illustrates the fact that the decrease in available surface per particle with increase in size is compensated by the increase in maximum PEI packing density. Interestingly, electrophoresis data indicates that PEI_{25}–$SiNP_{100}$ and PEI_{25}–$SiNP_{50}$ bind more DNA than PEI_{25}–$SiNP_{200}$ and PEI_{25}–$SiNP_{400}$. However, higher transfection is obtained for PEI_{25}–$SiNP_{50}$ and PEI_{25}–$SiNP_{200}$. This strongly suggests that transfection efficiency is not directly related to PEI amount or particle size. A more relevant parameter is DNA compaction that depends on PEI conformation. Here $SiNP_{50}$ and $SiNP_{200}$ have similar transfection efficiency although $SiNP_{50}$ has lower PEI density but binds more DNA than $SiNP_{200}$. That is to say, the PEI chains on $SiNP_{50}$ are more effective for binding DNA than the PEI chain on $SiNP_{200}$. As mentioned above, this can be explained by considering that for small radius of curvature (i.e., large particles), PEI can adopt a flat configuration that is not favorable for DNA compaction. As the radius of curvature increases (i.e., the particle size decrease), PEI chains can adopt a more compact configuration to optimize their packing on the surface, a situation that is more favorable for DNA compaction.

Effect of PEI Molecular Weight on Fibroblast Transfection in 2D. With their limited tendency to aggregate and high PEI loading taken into account, the $SiNP_{200}$ particles were selected for the following investigations. For these $SiNP_{200}$ particles, decreasing the PEI molecular weight from 25 kDa to 10 kDa led to an increase of particle size polydispersity and an increase in the amount of adsorbed polymer (Table 2). For short PEI chains (MW = 1.8 kDa), submicronic aggregates were detected by DLS in PBS, whereas the amount of adsorbed PEI was similar to that of PEI_{25}. Large branched PEI chains are known to adopt a compact conformation whose dimensions decrease with decreasing MW.[34] This allows for a higher density of PEI molecules on the surface, explaining the higher rate of adsorption of PEI_{10} compared to PEI_{25}. However, when further decreasing the polymer MW, short chains can adopt a more linear conformation and a flat configuration on the surface, leading to a lower density and therefore a lower amount of adsorbed PEI. The observation of a significant aggregation of the $PEI_{1.8}$-$SiNP_{200}$ confirms this hypothesis, as flat PEI chains are less effective in improving colloidal stability via steric repulsion compared to extended conformations.[35]

Table 2. Diameter (d) and Zeta Potential (ζ) and PEI Amount for 200 nm Silica Nanoparticles after Coating with PEI of Different Molecular Weights (MW)

MW [kDa]	d_{PBS} [nm][a]	ζ_{PBS} [mV]	PEI [wt %][b]
1.8	>1000	+20 ± 12	15
10	310 ± 100	+19 ± 8	25
25	250 ± 40	+19 ± 6	15

[a]from DLS. [b]±2 wt %, from elemental analysis.

Agarose gel experiments performed on pDNA-complexed PEI-coated particles showed that the optimal plasmid:particle weight ratio was 1:30 w/w% independently of the PEI molecular weight, in agreement with the fact that a similar ζ value of +20 mV was found for all PEI-$SiNP_{200}$ particles (Figure 3).

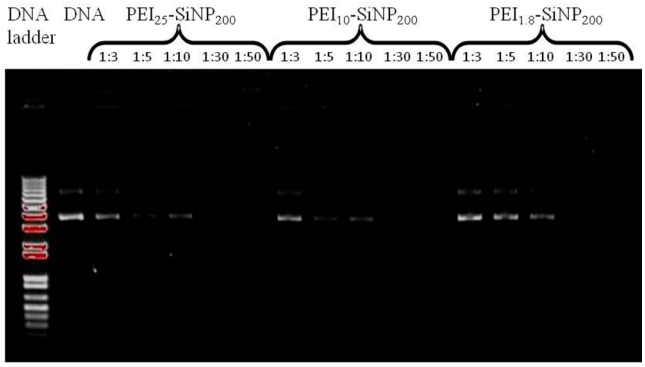

Figure 3. Agarose gel electrophoresis showing the PEI molecular weight influence on PEI-$SiNP_{200}$/pDNA complexation. A constant amount of DNA was complexed with silica particles at different weight ratios 1:3, 1:5, 1:10, 1:30, and 1:50.

Transfection assays in 2D revealed an interesting phenomenon (Figure 4). When PEI polymers alone were used as complexation reagents, an increase in transfection efficiency with increasing molecular weight was observed, in agreement with the literature.[11,36,37] When PEI-$SiNP_{200}$ systems were used, the optimal transfection was achieved with PEI_{10}.

DOI: 10.1021/am507389q
ACS Appl. Mater. Interfaces 2015, 7, 2503–2511

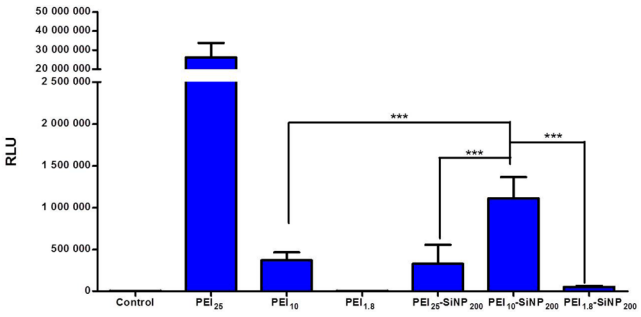

Figure 4. Transfection of 3T3 mouse fibroblasts after 4 h incubation with free and $SiNP_{200}$ coated with PEI of various molecular weights (n = 6). Variance of the luciferase expression between groups PEI_{10}, PEI_{25}-$SiNP_{200}$, $PEI_{1.8}$-$SiNP_{200}$ and group PEI_{10}-$SiNP_{200}$ was determined by one-way ANOVA with Dunnett posthoc test (*** P < 0.001).

Moreover, the particles showed a higher transfection efficiency than the polymer alone. This beneficial influence of PEI adsorption was further evidenced at lower molecular weight since $PEI_{1.8}$ alone did not show any transfection capability, whereas expression of luciferase was detectable for $PEI_{1.8}$-$SiNP_{200}$.

Whereas the higher amount of adsorbed PEI_{10} compared to PEI_{25} may, at least partially, account for the behavior of the corresponding particles, the observed improvement of transfection efficiency of shorter PEI upon coating suggests that another parameter should be considered. Importantly, the decrease in transfection efficiency of PEI chains with lower molecular weight was attributed to their decreased ability to compact DNA, a prerequisite to its internalization. Thus, based on our observation of particle aggregation upon plasmid addition, it is possible to assume that several particles are jointly involved in the compaction of one pDNA chain, allowing for its better compaction. Noticeably, such an aggregation process is known to be responsible for the transfection capabilities of cationic liposomal formulations (lipofection).[38]

To clarify the transfection pathway of PEI-coated SiNPs, FITC-containing silica nanoparticles were prepared and their internalization after complexation with pDNA by fibroblast cells was followed by fluorescence microscopy. As shown in Figure 5, the presence of silica particles (green fluorescence)

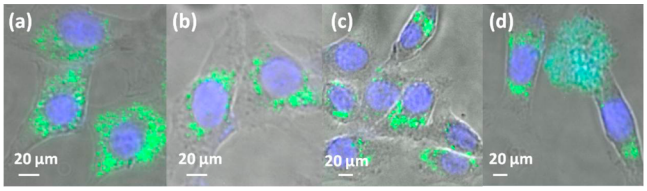

Figure 5. Fluorescence microscopy images showing internalization of (a) pDNA-$SiNP_{200}$, (b) pDNA-PEI_{25}-$SiNP_{200}$, (c) pDNA-PEI_{10}-$SiNP_{200}$, and (d) pDNA-$PEI_{1.8}$-$SiNP_{200}$ complexes by 3T3 fibroblasts after 24 h of incubation. Green fluorescence corresponds to FITC-labeled particles and blue to DAPI nuclei staining (scale bar = 20 μm).

within the cells and accumulating near the nucleus (blue fluorescence) was ascertained. Noticeably, significant particle aggregation was observed for $PEI_{1.8}$-$SiNP_{200}$, in agreement with the DLS data. Bare $SiNP_{200}$ nanoparticles put in contact with pDNA were also used as controls, showing a similar uptake as PEI-coated ones, in agreement with the literature.[39] Therefore, it is not possible to determine whether internalized particles bear PEI and pDNA or not. However, solutions containing the pDNA-PEI-$SiNP_{200}$ particles were regularly centrifuged and the absence of luciferase expression using the supernatant was checked. This evidences that transfection is not due to soluble pDNA-PEI complexes that may have been desorbed from the silica particle surface (Figure S2 in Supporting Information).

Altogether, these data indicate that PEI-coated silica nanoparticles ca. 200 nm in diameter are well-suited for plasmid delivery to fibroblast cells in 2D. Importantly, they are revealed to be even more effective than PEI alone when using low-molecular-weight polymers. This is a very interesting result as the cytoxicity of PEI is know to increase with its molecular weight due to higher cationic charge. Here, for all experiments carried out, cells showed good viability even when PEI alone was used as the pDNA carrier (Figure S3 in the Supporting Information). This is probably due to the small amount of PEI (2 μg/mL) used in these experiments together with the fact that 3T3 mouse fibroblast is a robust cell line. To study this point further, the viability of fibroblasts after 4 h of contact with PEI and PEI-coated SiNP200 particles as a function of dose (0−100 μg/mL) was studied (Figure 6). PEI_{25} showed

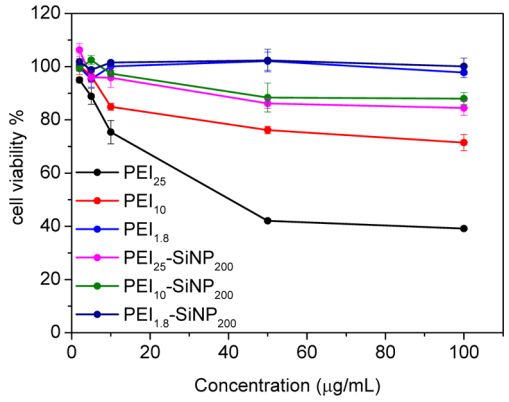

Figure 6. Impact of PEI and PEI-coated $SiNP_{200}$ nanoparticles after 4 h of contact as monitored by the Alamar Blue viability test.

significant cytotoxicity (i.e., cell viability <80%) above a 10 μg/mL concentration. This toxic dose increased to 50 μg/mL for PEI_{10} while no significant cytotoxicity was observed for $PEI_{1.8}$ in the studied concentration range. Strikingly, PEI_{25}-$SiNP_{200}$ and PEI_{10}-$SiNP_{200}$ showed a very limited impact on cell viability (>90%) at all investigated doses. This clearly demonstrates the beneficial effect of PEI adsorption on the silica nanoparticle surface on its cytotoxicity. As indicated earlier, this can be attributed to the fact that the apparent positive charge of the PEI chain is decreased by interaction of some of the protonated amine groups with the silica surface.

Cellularized Collagen Hydrogels as Models for 3D Transfection. Cellularized collagen hydrogels can be considered a good model of dermis to evaluate biomolecule effects in more physiologically relevant 3D conditions. pDNA-PEI-$SiNP_{200}$ particles were placed onto hydrogels to assess their diffusion through the collagen network and their ability to transfect immobilized 3T3 fibroblasts, using pDNA-PEI polyplexes as controls (model 1). For PEI_{25}-based polyplexes, an efficient transfection was detected from day 2 until the end of the experiment. In contrast, no luciferase expression was detected at day 2 when PEI_{25} was absorbed onto $SiNP_{200}$. The transfection became significant after day 5 only and was

DOI: 10.1021/am507389q
ACS Appl. Mater. Interfaces 2015, 7, 2503−2511

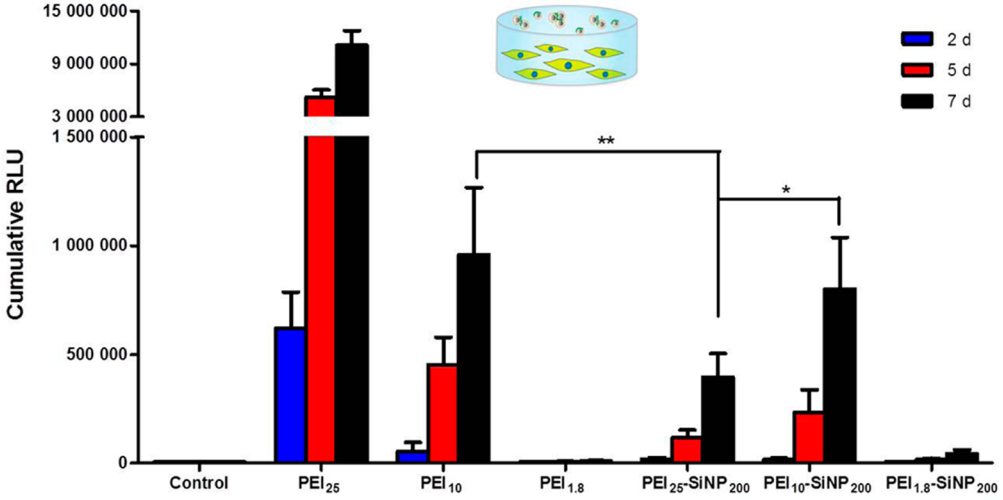

Figure 7. Transfection of 3T3 mouse fibroblasts immobilized in collagen hydrogels after 2, 5, and 7 d of contact with diffused free and $SiNP_{200}$-associated PEI of various molecular weights (model 1, $n = 6$). Variances among the cumulative luciferase expression on 7 d of PEI_{10}, PEI_{25}-$SiNP_{200}$, and PEI_{10}-$SiNP_{200}$ were determined by one-way ANOVA with Tukey posthoc test (*$P < 0.05$, ** $P < 0.01$).

enhanced after day 7 but remained 1 order of magnitude lower than the pDNA-PEI_{25} polyplexe alone (Figure 7). A similar trend was observed for PEI_{10} except that, after day 7, the particles showed a level of luciferase expression similar to the polyplexes. In the case of $PEI_{1.8}$, a weak transfection was detected at day 7 but only for particles. Overall, similar transfection efficiencies were obtained in these 3D models compared to the 2D configuration, except for a delay in luciferase expression. This is in good agreement with our recent study showing that silica nanoparticles with sizes ranging from 10 to 200 nm can diffuse through cellularized hydrogels, with the diffusion rate decreasing with increasing particle size.[40] Moreover, these particles could be internalized by immobilized fibroblasts. Interestingly, these data also suggest that the particle aggregates that were suggested to be responsible for pDNA compaction are preserved during diffusion.

Evaluation of Cellularized Nanocomposites as Cell Factories. Two different configurations for the use of plasmid-loaded particles associated with collagen hydrogels can be envisioned. The first strategy relies on the implantation of cellularized scaffolds incorporating the functional nanoparticles (model 2, Figure 8a). The advantage of this configuration is that DNA cargos can rapidly transfect cells encapsulated in the implant. Cells start to produce the biomolecules of interest in a short span of time. With this strategy, we can produce a cell factory to promote wound healing. In addition, the implantation of collagen hydrogels in the wound bed limits the risk of infection while preventing dehydration.[41,42] However, in this situation, it is important to check that particle internalization by the cells is still possible within the hydrogel. For this purpose, collagen hydrogels encapsulating both 3T3 fibroblasts and pDNA-PEI-$SiNP_{200}$ were prepared. Using fluorescent carriers, it was possible to observe the accumulation of particles within immobilized cells (Figure 8b–d).

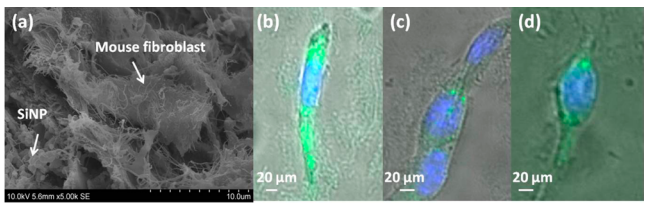

Figure 8. (a) SEM image of nanocomposites, displaying SiNP and fibroblast immobilized in collagen scaffold. Fluorescence microscopy image showing internalization of (b) pDNA-PEI_{25}-$SiNP_{200}$, (c) pDNA-PEI_{10}-$SiNP_{200}$, and (d) pDNA-$PEI_{1.8}$-$SiNP_{200}$ complexes by 3T3 fibroblasts within collagen hydrogels after 48 h of incubation, in which green fluorescence corresponds to FITC-labeled particles and blue to DAPI nuclei staining (scale bar = 20 μm).

Transfection assays performed in collagen hydrogels encapsulating both 3T3 fibroblasts and pDNA-PEI or pDNA-PEI-$SiNP_{200}$ also confirm internalization and gene expression (Figure 9). The luciferase expression followed similar trends in terms of the effect of PEI chain length, both as such or associated with $SiNP_{200}$ particles, compared to the complexes in solution. The main difference between the two systems lies on the lower expression rate for encapsulated complexes, suggesting that more vectors can enter into contact with the cells upon diffusion than after immobilization. We have previously shown that silica nanoparticles entrapped within the fibrillar collagen network are in close interaction with protein fibrils.[31] As a consequence, nanoparticles are expected to have restricted mobility. The alternative possibility is that cells proliferate and migrate within the collagen network, meet complexes, and internalize them.[26,27] This assumption is supported by the measured proliferation of fibroblasts within the hydrogels (Figure S4 in Supporting Information). The time needed for cell proliferation and migration can explain the observed delay in luciferase expression compared to the 2D situation. Nevertheless, the trends obtained for these nanocomposites as a function of PEI molecular weight and adsorption are in good agreement with that obtained for 2D transfection as well as for particle diffusion assays (model 1). This indicates that the pDNA-PEI-$SiNP_{200}$ complexes preserve their integrity upon encapsulation.

Importantly, no evidence for cytotoxicity was observed for model 1 and model 2 after 24 h of contact with PEI and PEI-coated particles during transfection experiments (Figure S5 in Supporting Information). Increasing the dose to 50 μg/mL showed high cytotoxicity for PEI_{25} and PEI_{10}, whereas coated silica nanoparticles had a limited impact on cell viability.

DOI: 10.1021/am507389q
ACS Appl. Mater. Interfaces 2015, 7, 2503−2511

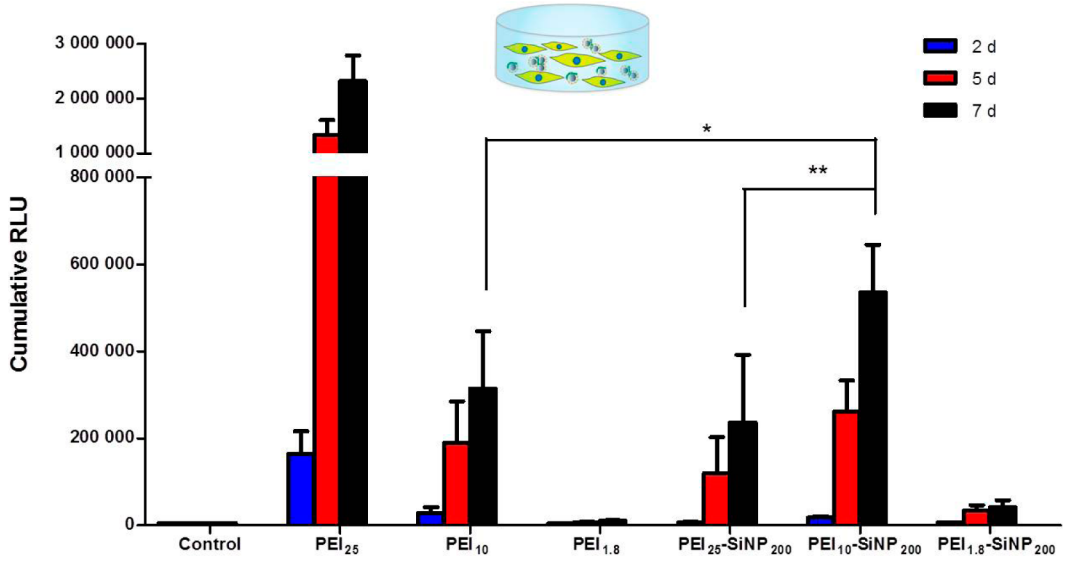

Figure 9. Transfection of 3T3 mouse fibroblasts coimmobilized with free and $SiNP_{200}$-associated PEI of various molecular weights in collagen hydrogels after 2, 5, and 7 d of incubation (model 2, $n = 6$). Variance among the cumulative luciferase expression on 7 d of PEI_{10}, PEI_{25}-$SiNP_{200}$, and PEI_{10}-$SiNP_{200}$ was determined by one-way ANOVA with Tukey posthoc test (*$P < 0.05$, ** $P < 0.01$).

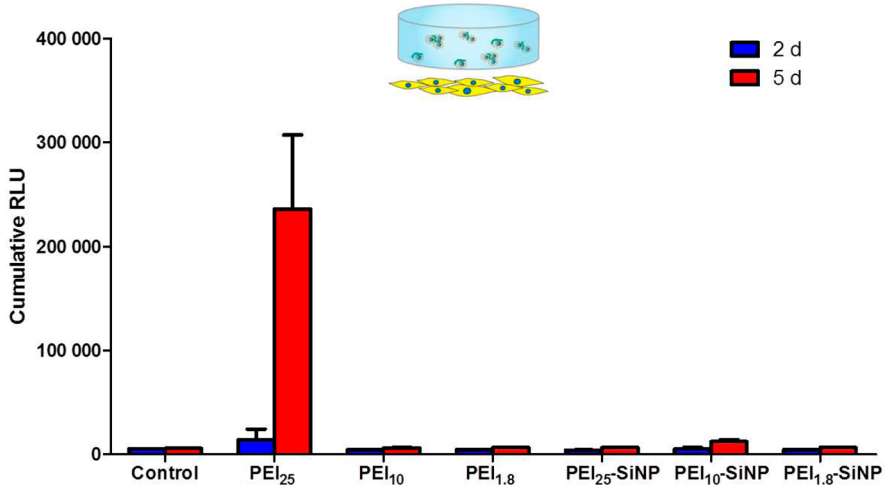

Figure 10. Transfection of 3T3 mouse fibroblasts in contact with free-floating collagen hydrogels containing free and $SiNP_{200}$-associated PEI of various molecular weight after 2, 5, and 7 d of incubation (model 3, $n = 3$).

Evaluation of Nanocomposites as Gene Delivery Systems. We then studied a second situation where the collagen scaffolds incorporating functional nanoparticles could act as a medicated dressing to deliver genes to tissue cells at the site of implantation. To test this configuration, hydrogels containing p-DNA-PEI or pDNA-PEI-$SiNP_{200}$ were left free-floating in the culture medium covering 3T3 cell-seeded well plates (model 3). As shown in Figure 10, a significant level of luciferase expression was only observed for pDNA-PEI25 after 5 days, but this level remains 1 order of magnitude below the transfection efficiency achieved in model 2. This strongly supports the hypothesis that entrapped vectors have a very limited mobility within the collagen hydrogels so that internalization is possible only if cells can migrate inside the protein network. One important outcome of this study is that complexing DNA with PEI-SiNP provides an efficient method to confine gene expression within the scaffold and avoid plasmid and silica particle dissemination in the surrounding tissue, at least before colonization of the material by host cells.

Implication in Gene Delivery and Tissue Engineering. Coupling PEI with plain spherical SiNP seems to be a very interesting strategy for targeted cell transfection. The cytocompatibility of SiNPs has been widely studied and discussed in the literature. Dissolution of silica nanoparticles into silicic acid has been demonstrated both in cells and in animals.[40,43] The spherical shape of SiNPs is also an important factor. Although needles or rods have the most appropriate shape to be engulfed by fibroblasts, they are more cytotoxic as they inflict mechanical damage when they penetrate biological membrane.[11,44,45] Moreover, spheres are more suitable to favor gene expression as they approach the nucleus more rapidly than elliptical particles.[45] Noticeably, most previous attempts to use silica nanoparticles as gene carriers have been made using mesoporous nanoparticles (MSNs). Regular MSNs are not good carriers of plasmidic DNA because of their small pores (2 nm) that prevent internal plasmid diffusion and compaction.[18] As a consequence, pDNA is stuck at the surface and is not protected against cellular nucleases. To overcome this problem,

DOI: 10.1021/am507389q
ACS Appl. Mater. Interfaces 2015, 7, 2503−2511

MSNs with ultralarge pores (23 nm) have been prepared.[21,46] These particles were able to pack pDNA and succeeded in transfecting cells. Alternatively, MSNs loaded with an anticancer drug were coated with PEI allowing for DNA and siRNA conjugation and delivery.[11] Our approach has the advantage of technical simplicity and short reaction time. Moreover, the possibility to encapsulate active drugs within Stöber particles has already been demonstrated so that the combination of drug and gene delivery using such plain SiNPs appears feasible.[31]

Considering the applications of the nanocomposites described here, it is important to first point out that tissue repair involves the formation of new healthy tissue in the wound site requiring several well-orchestrated phases to guide the tissue formation. Inflammation is crucial for the debridement of necrotic tissue and to kill bacteria. In the absence of modulation, chronic inflammation can occur.[1] The incorporation of a therapeutic gene modulating inflammation such as IL-10 within collagen nanocomposites could be useful to promote wound healing. In addition, inflammatory cells that infiltrate the implant could be directed toward a wound healing phenotype instead of an inflammatory one. Synthetic matrices made from biodegradable polymers such as PLGA or polycaprolactone were previously evaluated for gene delivery.[25,47] DNA/PEI complexes are mixed with the polymer in solution before matrix synthesis. In this case, polyplexes are encapsulated within material walls. This allows for a controlled and sustained delivery of polyplexes but requires a large porosity for cell infiltration. Moreover, synthetic polymers are not the natural support of fibroblasts and are not remodeled by cells. Alternatively, several collagen based-materials have been developed. Most of them are cross-linked collagen sponges rehydrated with a polyplexes solution (Transfecting reagent/pDNA). Polyplexes therefore adhere to the sponge wall and easily detach under flow. As a consequence, a rapid diffusion of polyplexes occurs preventing precise spatiotemporal control of the gene delivery process.[48] In this perspective, the silica-collagen materials combine several advantages. As demonstrated earlier, the stiffness of collagen hydrogels at 1 mg.mL^{-1} promotes fibroblast proliferation over 1 week and favors cell infiltration thanks to a pore size of ca. 5 μm.[49] This is highly beneficial to the target application as proliferating cells are more willing to be transfected than quiescent ones.[6] The other major advantage of the nanocomposites approach is that the DNA-loaded particles cannot diffuse out of the hydrogel. Therefore, in the first period after implantation, the delivery of plasmids to the immobilized cells would allow for the production and release of proteins. In a second phase, silica-collagen hydrogels will be colonized by inflammatory and connective cells.[30] Our data suggest that cells from the host organism could also be transfected during implant infiltration. Overall, it should allow for a prolonged production and delivery of active proteins at the implantation site and in its surroundings, favoring neotissue formation.

CONCLUSIONS

We demonstrate that PEI-coated plain silica nanoparticles are able to deliver therapeutic genes in a controlled and sustained manner within collagen hydrogels. The gene delivery properties of these particles were evidenced when they are transported through preformed cellularized hydrogels or coentrapped with fibroblasts, whereas no transfection was observed for cells external to the material. This offers various safe options to combine silica and collagen to design gene delivery systems promoting wound healing. In particular, the nanocomposite forms containing fibroblasts could be used as a cell factory to produce biomolecules, such as PDGF or IL-10, in a prolonged manner. Simultaneous encapsulation of silica particles containing additional active molecules, such as antibiotics, can also be envisioned, opening the route to highly modular bioactive medical dressing.

ASSOCIATED CONTENT

Supporting Information

Conditions of SiNP preparation (Table S1), TEM image of SiNP with different sizes (Figure S1), control transfection experiments with particle supernatant (Figure S2), cell viability test in 2D (Figure S3), proliferation of cells in collagen gel (Figure S4), and viability tests in 3D (Figure S5). This material is available free of charge via the Internet at http://pubs.acs.org.

AUTHOR INFORMATION

Corresponding Authors

*E-mail: thibaud.coradin@upmc.fr (T.C.).
*E-mail: christophe.helary@upmc.fr (C.H.).

Author Contributions

The manuscript was written through contributions of all authors. All authors have given approval to the final version of the manuscript. Christophe Hélary and Thibaud Coradin were equally responsible for this work.

Notes

The authors declare no competing financial interest.

ACKNOWLEDGMENTS

The authors thank C. Illoul, B. Haye, and G. Mosser (LCMCP) for technical assistance and S. Quignard (ENS, Paris) for fruitful discussions. X.W. PhD grant was funded by the China Scholarship Council.

REFERENCES

(1) Eming, S. A.; Krieg, T.; Davidson, J. M. Inflammation in Wound Repair: Molecular and Cellular Mechanisms. *J. Invest. Dermatol.* **2007**, *127*, 514−525.
(2) Boateng, J. S.; Matthews, K. H.; Stevens, H. N. E.; Eccleston, G. M. Wound Healing Dressings and Drug Delivery Systems: A review. *J. Pharm. Sci.* **2008**, *97*, 2892−2923.
(3) Menke, N. B.; Ward, K. R.; Witten, T. M.; Bonchev, D. G.; Diegelmann, R. F. Impaired Wound Healing. *Clin. Dermatol.* **2007**, *25*, 19−25.
(4) Bowen-Pope, D. F.; Malpass, T. W.; Foster, D. M.; Ross, R. Platelet-Derived Growth Factor In vivo: Levels, Activity, and Rate of Clearance. *Blood* **1984**, *64*, 458−469.
(5) Eppler, S. M.; Combs, D. L.; Henry, T. D.; Lopez, J. J.; Ellis, S. G.; Yi, J. H.; Annex, B. H.; McCluskey, E. R.; Zioncheck, T. F. A Target-Mediated Model to Describe the Pharmacokinetics and Hemodynamic Effects of Recombinant Human Vascular Endothelial Growth Factor in Humans. *Clin. Pharmacol. Ther.* **2002**, *72*, 20−32.
(6) Cam, C.; Segura, T. Matrix-Based Gene Delivery for Tissue Repair. *Curr. Opin. Biotechnol.* **2013**, *24*, 855−863.
(7) Place, E. S.; Evans, N. D.; Stevens, M. M. Complexity in Biomaterials for Tissue Engineering. *Nat. Mater.* **2009**, *8*, 457−470.
(8) Conwell, C. C.; Huang, L. Recent Advances in Non-Viral Gene Delivery. *Adv. Genet.* **2005**, *53*, 1−18.
(9) Eming, S. A.; Krieg, T.; Davidson, J. M. Gene Therapy and Wound Healing. *Clin. Dermatol.* **2007**, *25*, 79−92.
(10) Sun, J. Y.; Anand-Jawa, V.; Chatterjee, S.; Wong, K. K. Immune Responses to Adeno-Associated Virus and Its Recombinant Vectors. *Gene Ther.* **2003**, *10*, 964−976.

DOI: 10.1021/am507389q
ACS Appl. Mater. Interfaces 2015, 7, 2503−2511

(11) Xia, T.; Kovochich, M.; Liong, M.; Meng, H.; Kabehie, S.; George, S.; Zink, J. I.; Nel, A. E. Polyethyleneimine Coating Enhances the Cellular Uptake of Mesoporous Silica Nanoparticles and Allows Safe Delivery of siRNA and DNA Constructs. *ACS Nano* **2009**, *3*, 3273−3286.
(12) Dufes, C.; Uchegbu, I. F.; Schatzlein, A. G. Dendrimers in Gene Delivery. *Adv. Drug Delivery Rev.* **2005**, *57*, 2177−2202.
(13) Mintzer, M. A.; Grinstaff, M. W. Biomedical Applications of Dendrimers: A Tutorial. *Chem. Soc. Rev.* **2011**, *40*, 173−190.
(14) Boussif, O.; Lezoualc'h, F.; Zanta, M. A.; Mergny, M. D.; Scherman, D.; Demeneix, B.; Behr, J. P. A Versatile Vector for Gene and Oligonucleotide Transfer into Cells in Culture and in vivo: Polyethylenimine. *Proc. Natl. Acad. Sci. U. S. A.* **1995**, *92*, 7297−7301.
(15) Remy, J. S.; Abdallah, B.; Zanta, M. A.; Boussif, O.; Behr, J. P.; Demeneix, B. Gene Transfer with Lipospermines and Polyethylenimines. *Adv. Drug Delivery Rev.* **1998**, *30*, 85−95.
(16) Petersen, H.; Fechner, P. M.; Martin, A. L.; Kunath, K.; Stolnik, S.; Roberts, C. J.; Fischer, D.; Davies, M. C.; Kissel, T. Polyethylenimine-graft-Poly(ethylene glycol) Copolymers: Influence of Copolymer Block Structure on DNA Complexation and Biological Activities as Gene Delivery System. *Bioconjugate Chem.* **2002**, *13*, 845−854.
(17) Hu, C.; Peng, Q.; Chen, F.; Zhong, Z.; Zhuo, R. Low Molecular Weight Polyethylenimine Conjugated Gold Nanoparticles as Efficient Gene Vectors. *Bioconjugate Chem.* **2010**, *21*, 836−843.
(18) Mamaeva, V.; Sahlgren, C.; Linden, M. Mesoporous Silica Nanoparticles in Medicine-Recent Advances. *Adv. Drug Delivery Rev.* **2013**, *65*, 689−702.
(19) Meng, H.; Xue, M.; Xia, T.; Ji, Z.; Tarn, D. Y.; Zink, J. I.; Nel, A. E. Use of Size and a Copolymer Design Feature To Improve the Biodistribution and the Enhanced Permeability and Retention Effect of Doxorubicin-Loaded Mesoporous Silica Nanoparticles in a Murine Xenograft Tumor Model. *ACS Nano* **2011**, *5*, 4131−4144.
(20) Kim, T.-W.; Slowing, I. I.; Chung, P.-W.; Lin, V. S.-Y. Ordered Mesoporous Polymer−Silica Hybrid Nanoparticles as Vehicles for the Intracellular Controlled Release of Macromolecules. *ACS Nano* **2010**, *4*, 360−366.
(21) Kim, M.-H.; Na, H.-K.; Kim, Y.-K.; Ryoo, S.-R.; Cho, H. S.; Lee, K. E.; Jeon, H.; Ryoo, R.; Min, D.-H. Facile Synthesis of Monodispersed Mesoporous Silica Nanoparticles with Ultralarge Pores and Their Application in Gene Delivery. *ACS Nano* **2011**, *5*, 3568−3576.
(22) Rosenholm, J. M.; Duchanoy, A.; Lindén, M. Hyperbranching Surface Polymerization as a Tool for Preferential Functionalization of the Outer Surface of Mesoporous Silica. *Chem. Mater.* **2007**, *20*, 1126−1133.
(23) Buchman, Y. K.; Lellouche, E.; Zigdon, S.; Bechor, M.; Michaeli, S.; Lellouche, J.-P. Silica Nanoparticles and Polyethyleneimine (PEI)-Mediated Functionalization: A New Method of PEI Covalent Attachment for siRNA Delivery Applications. *Bioconjugate Chem.* **2013**, *24*, 2076−2087.
(24) Luo, D.; Han, E.; Belcheva, N.; Saltzman, W. M. A Self-assembled, Modular DNA Delivery System Mediated by Silica Nanoparticles. *J. Controlled Release* **2004**, *95*, 333−341.
(25) Shea, L. D.; Smiley, E.; Bonadio, J.; Mooney, D. J. DNA Delivery From Polymer Matrices for Tissue Engineering. *Nat. Biotechnol.* **1999**, *17*, 551−554.
(26) Grinnell, F. Fibroblast Biology in Three-Dimensional Collagen Matrices. *Trends Cell Biol.* **2003**, *13*, 264−269.
(27) Grinnell, F.; Petroll, W. M. Cell Motility and Mechanics in Three-Dimensional Collagen Matrices. *Annu. Rev. Cell Dev. Biol.* **2010**, *26*, 335−361.
(28) De Laporte, L.; Shea, L. D. Matrices and Scaffolds for DNA Delivery in Tissue Engineering. *Adv. Drug Delivery Rev.* **2007**, *59*, 292−307.
(29) Gojgini, S.; Tokatlian, T.; Segura, T. Utilizing Cell−Matrix Interactions To Modulate Gene Transfer to Stem Cells Inside Hyaluronic Acid Hydrogels. *Mol. Pharmaceutics* **2011**, *8*, 1582−1591.
(30) Desimone, M. F.; Helary, C.; Quignard, S.; Rietveld, I. B.; Bataille, I.; Copello, G. J.; Mosser, G.; Giraud-Guille, M. M.; Livage, J.; Meddahi-Pelle, A.; Coradin, T. In Vitro Studies and Preliminary In Vivo Evaluation of Silicified Concentrated Collagen Hydrogels. *ACS Appl. Mater. Interfaces* **2011**, *3*, 3831−3838.
(31) Alvarez, G. S.; Helary, C.; Mebert, A. M.; Wang, X. L.; Coradin, T.; Desimone, M. F. Antibiotic-loaded Silica Nanoparticle-Collagen Composite Hydrogels with Prolonged Antimicrobial Activity for Wound Infection Prevention. *J. Mater. Chem. B* **2014**, *2*, 4660−4670.
(32) Meszaros, R.; Thompson, L.; Varga, I.; Gilanyi, T. Adsorption Properties of Polyethyleneimine on Silica Surfaces in the Presence of Sodium Dodecyl Sulfate. *Langmuir* **2003**, *19*, 9977−9980.
(33) Wang, Z. J.; Tiruppathi, C.; Minshall, R. D.; Malik, A. B. Size and Dynamics of Caveolae Studied Using Nanoparticles in Living Endothelial Cells. *ACS Nano* **2009**, *3*, 4110−4116.
(34) Rejman, J.; Oberle, V.; Zuhorn, I. S.; Hoekstra, D. Size-Dependent Internalization of Particles via the Pathways of Clathrin- and Caveolae-Mediated Endocytosis. *Biochem. J.* **2004**, *377*, 159−169.
(35) Wightman, L.; Kircheis, R.; Rossler, V.; Carotta, S.; Ruzicka, R.; Kursa, M.; Wagner, E. Different Behavior of Branched and Linear Polyethylenimine for Gene Delivery In Vitro and In Vivo. *J. Gene Med.* **2001**, *3*, 362−372.
(36) Godbey, W. T.; Wu, K. K.; Mikos, A. G. Poly(ethylenimine) and Its Role in Gene Delivery. *J. Controlled Release* **1999**, *60*, 149−160.
(37) Godbey, W. T.; Ku, K. K.; Hirasaki, G. J.; Mikos, A. G. Improved Packing of Poly(ethylenimine)/DNA Complexes Increases Transfection Efficiency. *Gene Ther.* **1999**, *6*, 1380−1388.
(38) Felgner, P. L.; Gadek, T. R.; Holm, M.; Roman, R.; Chan, H. W.; Wenz, M.; Northrop, J. P.; Ringold, G. M.; Danielsen, M. Lipofection - a Highly Efficient, Lipid-Mediated DNA-Transfection Procedure. *Proc. Natl. Acad. Sci. U. S. A.* **1987**, *84*, 7413−7417.
(39) Quignard, S.; Mosser, G.; Boissière, M.; Coradin, T. Long-Term Fate of Silica Nanoparticles Interacting with Human Dermal Fibroblasts. *Biomaterials* **2012**, *33*, 4431−4442.
(40) Quignard, S.; Helary, C.; Boissiere, M.; Fullana, J.-M.; Lagree, P.-Y.; Coradin, T. Behaviour of Silica Nanoparticles in Dermis-Like Cellularized Collagen Hydrogels. *Biomater. Sci.* **2014**, *2*, 484−492.
(41) Powers, J. G.; Morton, L. M.; Phillips, T. J. Dressings for Chronic Wounds. *Dermatol. Ther.* **2013**, *26*, 197−206.
(42) Slaughter, B. V.; Khurshid, S. S.; Fisher, O. Z.; Khademhosseini, A.; Peppas, N. A. Hydrogels in Regenerative Medicine. *Adv. Mater.* **2009**, *21*, 3307−3329.
(43) Chen, K. H.; Zhang, J. X.; Gu, H. C. Dissolution from Inside: A Unique Degradation Behaviour of Core-Shell Magnetic Mesoporous Silica Nanoparticles and the Effect of Polyethyleneimine Coating. *J. Mater. Chem.* **2012**, *22*, 22005−22012.
(44) Ferrari, M. Beyond Drug Delivery. *Nat. Nanotechnol.* **2008**, *3*, 131−132.
(45) Kettiger, H.; Schipanski, A.; Wick, P.; Huwyler, J. Engineered Nanomaterial Uptake and Tissue Distribution: from Cell to Organism. *Int. J. Nanomed.* **2013**, *8*, 3255−3269.
(46) Gao, F.; Botella, P.; Corma, A.; Blesa, J.; Dong, L. Monodispersed Mesoporous Silica Nanoparticles with Very Large Pores for Enhanced Adsorption and Release of DNA. *J. Phys. Chem. B* **2009**, *113*, 1796−1804.
(47) Holladay, C.; Keeney, M.; Greiser, U.; Murphy, M.; O'Brien, T.; Pandit, A. A Matrix Reservoir for Improved Control of Non-Viral Gene Delivery. *J. Controlled Release* **2009**, *136*, 220−225.
(48) Jang, J. H.; Rives, C. B.; Shea, L. D. Plasmid Delivery In Vivo From Porous Tissue-Engineering Scaffolds: Transgene Expression and Cellular Transfection. *Mol. Ther.* **2005**, *12*, 475−483.
(49) Helary, C.; Bataille, I.; Abed, A.; Illoul, C.; Anglo, A.; Louedec, L.; Letourneur, D.; Meddahi-Pellé, A.; Giraud-Guille, M. M. Concentrated Collagen Hydrogels as Dermal Substitutes. *Biomaterials* **2010**, *31*, 481−490.

DOI: 10.1021/am507389q
ACS Appl. Mater. Interfaces 2015, 7, 2503−2511